RUSLE Model Based Annual Soil Loss Quantification for Soil Erosion Protection: A Case of Fincha Catchment, Ethiopia

Authors: Wagari, Meseret, and Tamiru, Habtamu

Source: Air, Soil and Water Research, 14(1)

Published By: SAGE Publishing

URL: https://doi.org/10.1177/11786221211046234

RUSLE Model Based Annual Soil Loss Quantification for Soil Erosion Protection: A Case of Fincha Catchment, Ethiopia

Air, Soil and Water Research
Volume 14: 1–12

DOI: 10.1177/11786221211046234

Meseret Wagari and Habtamu Tamiru
Wollega University, Ethiopia

ABSTRACT: In this study, Revised Universal Soil Loss Equation (RUSLE) model and Geographic Information System (GIS) platforms were successfully applied to quantify the annual soil loss for the protection of soil erosion in Fincha catchment, Ethiopia. The key physical factors such as rainfall erosivity (*R*-factor), soil erodibility (*K*-factor), topographic condition (LS-factor), cover management (*C*-factor), and support practice (*P*-factor) were prepared in GIS environment from rainfall, soil, Digital Elevation Model (DEM), Land use/Land cover (LULC) respectively. The RUSLE equation was used in raster calculator of ArcGIS spatial tool analyst. The individual map of the derived factors was multiplied in the raster calculator and an average annual soil loss ranges from 0.0 to 76.5 t ha^{-1} yr^{-1} was estimated. The estimated annual soil loss was categorized based on the qualitative and quantitative classifications as Very Low (0–15 t ha^{-1} yr^{-1}), Low (15–45 t ha^{-1} yr^{-1}), Moderate (45–75 t ha^{-1} yr^{-1}), and High (>75 t ha^{-1} yr^{-1}). It was found from the generated soil erosion severity map that about 45% of the catchment area was vulnerable to the erosion with an annual soil loss of (>75 t ha^{-1} yr^{-1}), and this demonstrates that the erosion reduction actions are immediately required to ensure the sustainable soil resources in the study area. The soil erosion severity map generated based on RUSLE model and GIS platforms have a paramount role to alert all stakeholders in controlling the effects of the erosion. The results of the RUSLE model can also be further considered along with the catchment for practical soil loss protection practices.

KEYWORDS: ArcGIS, catchment, qualitative classification, severity, key factors

TYPE: Advances in Spatial Modeling, Geostatistics, and Machine Learning in Soil Science - Original Research

CORRESPONDING AUTHOR: Meseret Wagari, Department of Natural Resources Management, Wollega University, P.O.B 395, Ethiopia. Email: meseret123wag@gmail.com

Background

The primary source of soil degradation is soil erosion. The impacts of soil erosion is very high where the environmental protection and management strategies are very weak (Thapa, 2020). The soil erosion can causes the reduction in agricultural productivity, ecosystem disturbances, and pollution of water (Li, 2018; Wubie & Assen, 2020). Physical and climatic features of a catchment such as topographic conditions, land use land cover (LULC), rainfall intensity, and the soil characteristics are the key significant factors of the soil erosion (Yan et al., 2018). The loss of the top fertile soil nutrients is intensely increasing due to this natural phenomenon (Chuenchum et al., 2020; Yesuph & Dagnew, 2019). As studies conducted in (Fernandez et al., 2003; Negasa, 2020; Panagos et al., 2018) indicate, the majority of the farmers in poor countries are facing the problem of expenditure to purchase artificial fertilizers to increase the yield. The intrusion of the surface runoff into the public water sources can invite damaging chemicals and pollutants (Hategekimana et al., 2020). Even though soil erosion is happening worldwide, its impacts are very high in poor countries due to the weakness of natural resources management (Markose & Jayappa, 2016). In Africa, soil erosion is one of the challenging natural phenomena that affecting the entire region. Ethiopia is no exception, as the entire region of the country is suffering from this problem (Yesuph & Dagnew, 2019). Researchers have been searching for effective tools and methods to quantify the total annual soil loss in a given catchment (Kayet et al., 2018; Shiferaw & Abebe, 2020). Universal Soil Loss Equation (USLE) and the Revised Universal Soil Loss Equation (RUSLE) are the most widely used soil loss estimation models (Bekele & Gemi, 2021). RUSLE uses an empirical equation and associates different physical and climatic features. Geographical Information System (GIS) and the data retrieved from remote sensing (RS) technology are integrated in GIS platform to quantify the soil loss (Kayet et al., 2018; Phinzi & Silas, 2019). In the current study area, the impacts and severity of soil erosion are intensively increasing and causing the depletion of top fertile soil and polluting the sources of public drinking water. The intensity of rainfall and surface dynamic changes such LULC, slope, and soil erodibility are also doubling the soil erosion potential. In Ethiopia, RUSLE model and GIS tools were used intensively to quantify the soil losses, generate soil erosion severity map, to generate soil erosion severity map, identify soil landscape variability (Bekele & Gemi, 2021; Dinka, 2020; Girmay et al., 2020). This study was conducted in Fincha Catchment where the soil is highly vulnerable to erosion; however, where such studies are not undertaken. RUSLE model and GIS platform were successfully applied to quantify the rate of annual soil loss and the soil erosion severity map under different classifications was generated to a better understanding of the spatial variability of the soil erosion in the study area.

Methods

Study area

This study area was conducted in the Fincha catchment, Abay Basin, Ethiopia as shown in Figure 1. This delineated watershed is geographically found between 37°0.06′00″E and 37°33′18″E longitude and 09°21′11″N to 10°01′00″N latitude

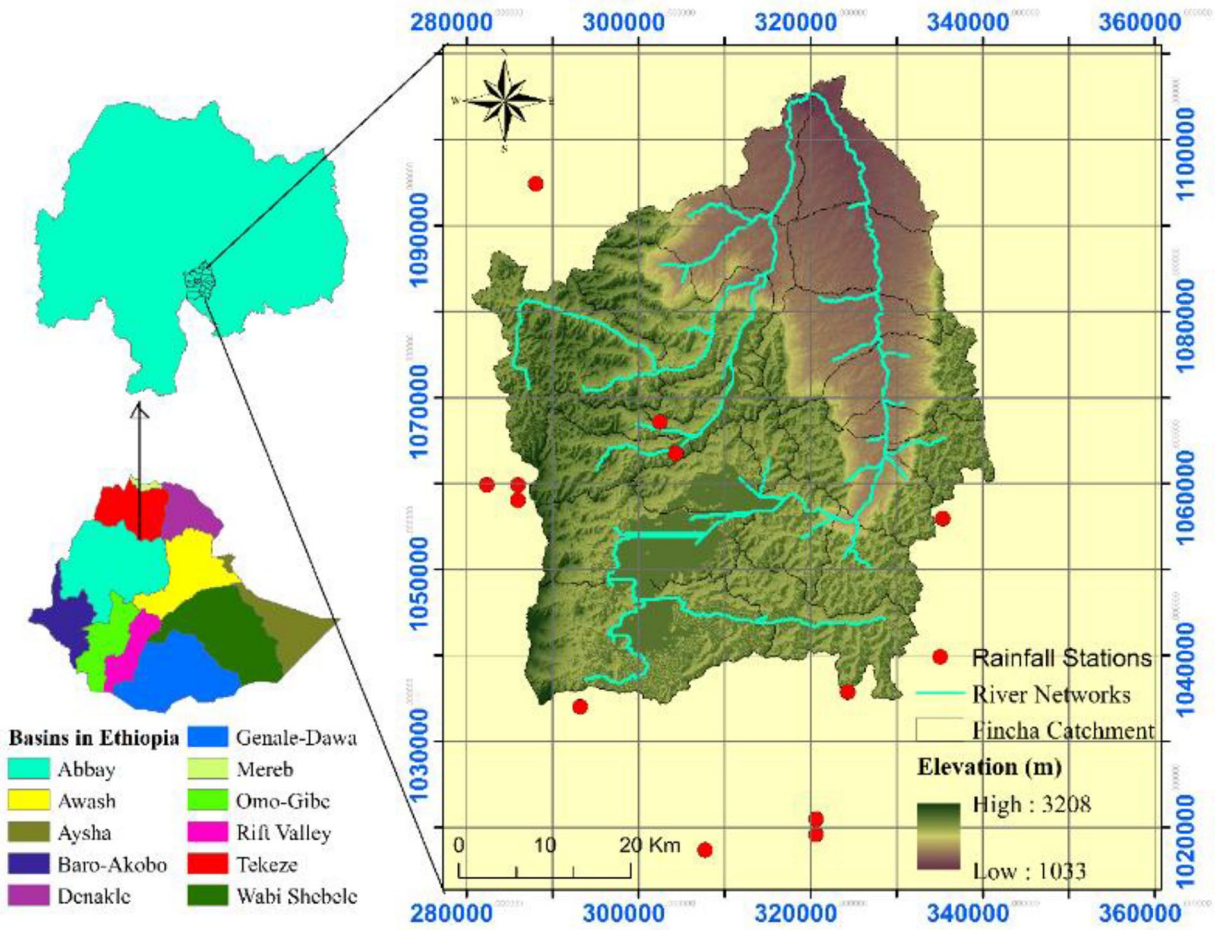

Figure 1. Geographical location of the study area.

and covers total area of 2148 ha. The major landforms fall in rolling terrain class (2%–10%) which covered about 46%, rolling terrain about 27%, and hilly terrain about 23%. Only small pockets of land which accounts about 1% from total area was covered by flat plain and 1% also characterized by highly rugged mountainous and rolled topography with steep slopes(Olika & Iticha, 2019). The meteorological (recorded precipitation) stations contributing to the outlet were identified using Thiessen Polygon. Accordingly, the contributing stations namely: *Alibo, Shambu, haro, Neshi, Homi, Hareto, Gabate, Kombolcha*, and *Wayu* were identified. Since the intensity of rainfall and the infiltration capacity of the soil, geologic, and hydrogeologic settings are the main causes for groundwater recharge, the exploration of potential zones considers the rainfall stations. The soils of the area were dominated by Haplic Vertisols, Eutric Cambisols, and Nitisols.

Data

To quantify the annual soil loss in the catchment, recorded rainfall of eleven (11) stations (Table 1), Digital Elevation Model (DEM), existing soil map, and LANDSAT imageries were used to derive the key factors of RUSLE model. The point-based recorded rainfall data of the selected stations were converted into areal rainfall using an advanced interpolation technique called Kriging method. For this purpose, spatial analyst tool in GIS environment was used to convert the point data into areal using an ordinary kriging method (equation (1)). The selected significant factors (R-factor, P-factor, K-factor, LS-factor, and C-factor) were derived from the areal rainfall, LULC, slope, and soil data. Rainfall, geology, and soil were obtained from Ethiopian Ministry of Water (MW) and LULC was generated from the LANDSAT imageries retrieved from https://earthexplorer.usgs.gov/ for the 2020 datasets. Digital Elevation Model (DEM) (12.5 × 12.5 m) was downloaded from Alaska University official website: https://search.asf.alaska.edu/.

$$\hat{Z}(X_o) = \sum_{i=1}^{N} \lambda_i Z(X_i) \quad (1)$$

Where $\hat{Z}(X_o)$ *and* $\hat{Z}(X_i)$ *are the interpolated values and observed values of the individual points, N is the total number of observations, and* λ_i *the weight of each observation.*

Soil loss models

A bunch of documents are available regarding the different soil loss models; however, RUSLE is effectively and intensively

Table 1. Rainfall Stations in and Surrounding Fincha Subbasin.

NO.	STATION NAME	LONG	LAT	ELEVATION (M)	ANNUAL MEAN PRECIPITATION (MM)
1	Alibo	37.0795	9.8904	2,405.53	1,754.2
2	Kewo	37.5543	9.8271	2,362.15	1,353.65
3	Jardega	37.0143	9.8065	2,402.98	2,030.93
4	Sombo	37.0326	9.7424	2,385.78	1,988.75
5	Dedu	37.5357	9.6889	2,270.19	1,491.6
6	Achane	37.3216	9.6547	2,398.33	1,645.81
7	Shambu	37.0943	9.5707	2,556.4	1,827.07
8	Fincha-a	37.362	9.5659	2,226.33	1,528.11
9	Kombolcha	37.4781	9.5097	2,390.25	1,621.3
10	Bila	37.0279	9.2925	2,114.34	1,728.16
11	Goben	37.311	9.1741	2,610.34	1,906.2

used (Fayas et al., 2019; Markose & Jayappa, 2016; Mengistu et al., 2016) worldwide in several catchments. The reliability and capability of RUSLE model was evaluated by (Prasannakumar et al., 2012), and it has been used in the catchment where the impact of soil erosion is very high. RUSLE model is the most popular soil loss estimation model that can be modeled in GIS platform. The raster calculator in spatial analyst tool of GIS environment can easily be used to estimate the rate of soil loss by combining the key significant factors.

Description of RUSLE model

RUSLE is an empirical erosion model recognized as an effective tool to quantify the mean annual soil losses and its risk (Chuenchum et al., 2020). This model is applicable for arable land and limited to a long-term rainfall record. The RUSLE model receives the physical features and surface dynamic changes such as *R*-factor, *P*-factor, *K*-factor, LS-factor, and C-factor as criteria for the quantification of annual soil loss. Based on the physical evidences, and availability of data in this catchment, the selected significant factors were prepared and used the RUSLE model (equation (2)) to estimate the annual soil loss. The raster calculator in the spatial analyst tool of GIS environment has a capability to generate the soil loss map, for this purpose, the flowchart showing the detailed procedures and data needed are summarized in Figure 2.

$$A = R * K * LS * C * P \quad (2)$$

Where A the total annual soil loss (t/ha per year), t is the thickness of lost soil
R Rainfall erosivity factor (MJmm ha^{-1} h^{-1} year^{-1})
K Soil erodibility factor (t haMJ^{-1} mm^{-1})
LS Slope length and steepness factor (dimensionless)
C Over and management factor (dimensionless)
P Support practice factor (dimensionless)

*Rainfall erosivity factor (*R*)*

Rainfall erosivity factor *R* describes the relationship between the rainfall intensity and the soil responses to it (Kayet et al., 2018). According to the information obtained from the national meteorology of Abay Basin in which the current study is found, varies from 1353.65 to 2030.93 mm. The rainfall erosivity factor (*R*) is an important factor of the RUSLE model to estimate the annual soil loss. The values of rainfall erosivity factor for this study was derived from fifteen (15) years recorded rainfall of 11 meteorological stations (Refer Table 1). Distributed rainfall in Kriging interpolation technique was used to generate the rainfall erosivity factor (*R*) (Dessalegn et al., 2017) using the empirical equation (Bekele & Gemi, 2021; Hategekimana et al., 2020) as shown in (equation (3)).

$$\boldsymbol{R} = 1.24 * \boldsymbol{P}^{1.36} \quad (3)$$

Where *R* Rainfall erosivity factor (MJmm ha^{-1} h^{-1} yr^{-1})
P Annual mean precipitation (mm)

*Soil erodibility factor (*K*)*

The soil erodibility factor (*K*) is a quantitative description of the susceptibility of soil to erosion. The degree of tolerating the effect of intensive rainfall is reached when soil particles are detached and transported. The cohesive force between the soil particles is the restoring force, and if the force due to the moving surface runoff is much greater than the cohesive force, the soil particles are exposed to erosion (Girmay et al., 2020; Seifu et al., 2020). The permeability of the soil and the degree of erodibility are interconnected parameters (Kayet et al., 2018). The ability of soil

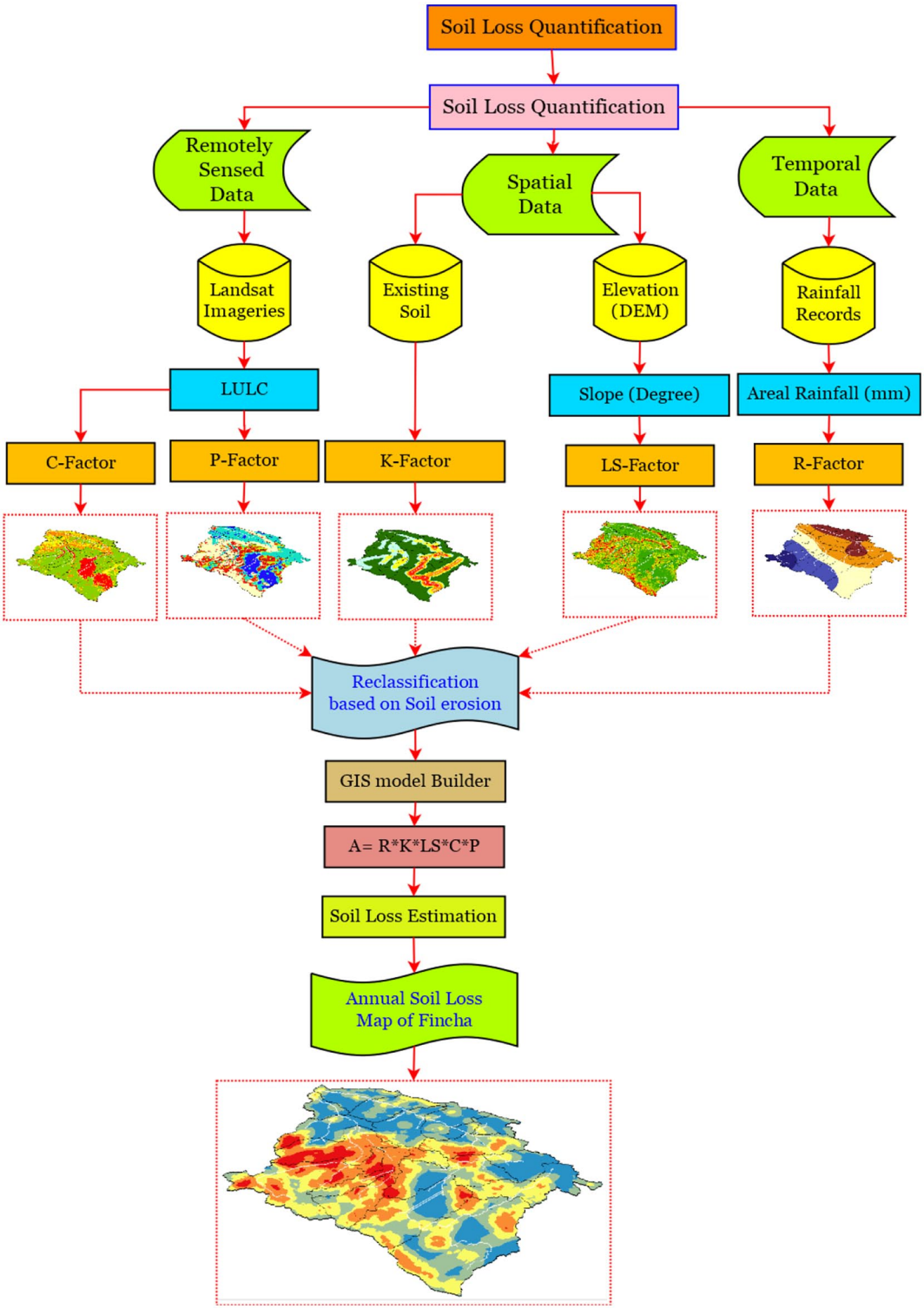

Figure 2. Detail flowchart of the steps and data needed in the study.

particles in persisting against rainfall is different in different soil types and this property is expressed in terms of erodibility factor (Ayenew et al., 2018). The soil types and the corresponding values of the erodibility factor (*K*) in the study area.

Topographic factor (LS)

The severity of the spatial variability of soil erosion relies on the topographic conditions of an area. The steepness or the flatness of an area governs the degree of the erodibility of soil particles. The speed of the water flowing over soil and the slope of the area are dependent parameters (Kayet et al., 2018). The length of the slope and slope steepness of the area in the study area was generated using Digital Elevation Model (DEM) of 12.5×12.5 m and LS-factor was generated in ArcGIS version 10.4. Flow accumulation and slope (%) are commonly used input parameters with a fixed cell size with regression equation(Abdulkadir et al., 2019) (Eq.4).

Table 2. Soil Types and Corresponding Erodibility Factor (*K*-Values) in the Catchment.

SOIL TYPES	*K*-FACTOR VALUE	AREA (KM^2)	AREA (%)
Chromic Luvisols	0.18	3.71	17.27
Eutric Cambisols	0.36	4.57	21.28
Eutric Leptosols	0.13	0.54	2.51
Eutric Vertisols	0.45	2.42	11.27
Haplic Alisols	0.27	8.58	39.94
Haplic Arenosols	0.19	0.25	1.16

$$LS = \left\{ Flow\ accumalation * \left(\frac{Cellsize}{23.13} \right) \right\}^{0.4} * \left\{ \frac{\sin\left(slope(\%) * 0.01745 \right)}{0.09} \right\}^{1.3} * 1.6 \quad (4)$$

Where LS Slope length and steepness factor (dimensionless)

*Support practice (*P*) and cover and Management factors(*C*)*

The impact of agricultural or cropping system and the practice of crop management on the rate of soil erosion is defined using the *C*-factor (Hategekimana et al., 2020). It also characterizes the influence of soil disturbing activities, plant sequence, and productivity level, soil cover and subsurface bio-mass on soil erosion. Cover and management factor is important in developing conservation plans (Mohamed & Shantha, 2019). The other key significant factor used in RUSLE model is the support and conservation practices factor called *P*-factor (Iticha & Takele, 2018). This parameter estimates the support and conservation practices and the corresponding to a particular support practice in up and down slope farming (Markose & Jayappa, 2016). LUC types are the primary inputs for the estimation of *P* and *C* values in a given catchment, and therefore in this study, for the LULC and the corresponding *C* and *P* values (Table 2 and Figure 3) were assigned based on their influences on soil erosion.

Results and discussion

Estimation of soil loss

In this study, the rate of annual soil loss ranging from 0 to 76.5 t ha^{-1} yr^{-1} was quantified sing RUSLE model and GIS tools. The total area of the study area is 21.48 km^2 (2148 ha) and the corresponding annual soil loss was estimated as164, 322 t ha^{-1} yr^{-1}. The vulnerability of soil to the erosion is very in this catchment as we can see from soil severity map generated in RUSLE model. The estimated annual soil loss (0 to 76.5 t ha^{-1} yr^{-1}) in this study was much higher than the total annual soil formation rate estimated by (Girmay et al., 2020) that ranges from 2 to 22 t ha^{-1} yr^{-1}. This indicates that the sensitivity to erosion is highly increased due to increment values of support practice and cover management practice factors. The surface dynamic change of the area should be managed and actions are important to control the LULC to minimize the volume of the surface runoff that in turn increases the erodibility of the soil. Rainfall erosivity factor (*R*-factor), soil erodibility factor (*K*-factor), support practices factor (*P*-factor), cover management practice (*C*-factor), and the topographic factor (LS-factor) derived from the existing data and detailed information about each factor were briefed in the next sections.

*Rainfall erosivity factor (*R*-factor)*

The rainfall intensity and the nature of the surface are the primary reasons for the soil erosion (Fayas et al., 2019). The speed of the surface runoff is governed by the slope of the area. The degree of the detachment of soil particles is dependent of rainfall erosivity. The classifications of the rainfall of the thematic maps in both approaches revealed almost the same categories. This indicates that the ANN model can also be used as an alternative in generating a thematic map. The rainfall in the study area was reclassified into five (5) major categories as (1,425.18–1,586.69 mm), (1,586.69–1,679.21 mm), (1,679.21–1,766.98 mm), (1,766.98–1,873.74 mm), and (1,873.74–2030.30 mm), and the corresponding rainfall erosivity were (0.00–1.34 MJmm ha^{-1} h^{-1} yr^{-1}), (1.34–3.42 MJmm ha^{-1} h^{-1} yr^{-1}), (3.42–5.96 MJmm ha^{-1} h^{-1} yr^{-1}), (5.96–8.83 MJmm ha^{-1} h^{-1} yr^{-1}), and (8.83–11.96 MJmm ha^{-1} h^{-1} $year^{-1}$) respectively. As we can see from Figure 4, the southwestern part of the catchment gets an annual rainfall ranging from 1,873.74–2030.30 mm, and there is high sensitivity to erosion. The values of the rainfall erosivity factor are also very high in the southwestern and middle portions of the catchment.

*Soil erodibility factor (*K*)*

Soil erodibility factor (*K*-factor) is one of the key parameters of soil erosion modeling that is commonly used in RUSLE model (Panagos et al., 2014). The relationship between the rainfall intensity and the ability of soil to erode is expressed as erodibility factor. Six (6) soil types namely: Chromic Luvisols, Eutric Cambisols, Eutric Leptosols, Eutric Vertisols, Haplic Alisols, and Haplic Arenosols with the corresponding percentage of coverage as 17.27%, 11.27%, 39.94%, 21.28%, 2.51%, and 1.16% were identified in this catchment. Of these soil groups, Eutric Leptosols and Eutric Vertisols cover about 61.22% of the entire region, and the erosion status is severe in these soil groups, which in turn indicates a high erodibility of the soil in the catchment (Fenta et al., 2020). The values of soil erodibility factor (K) ranging from 0.13 to 0.45 were estimated in the study area (Table 3 and Figure 5).

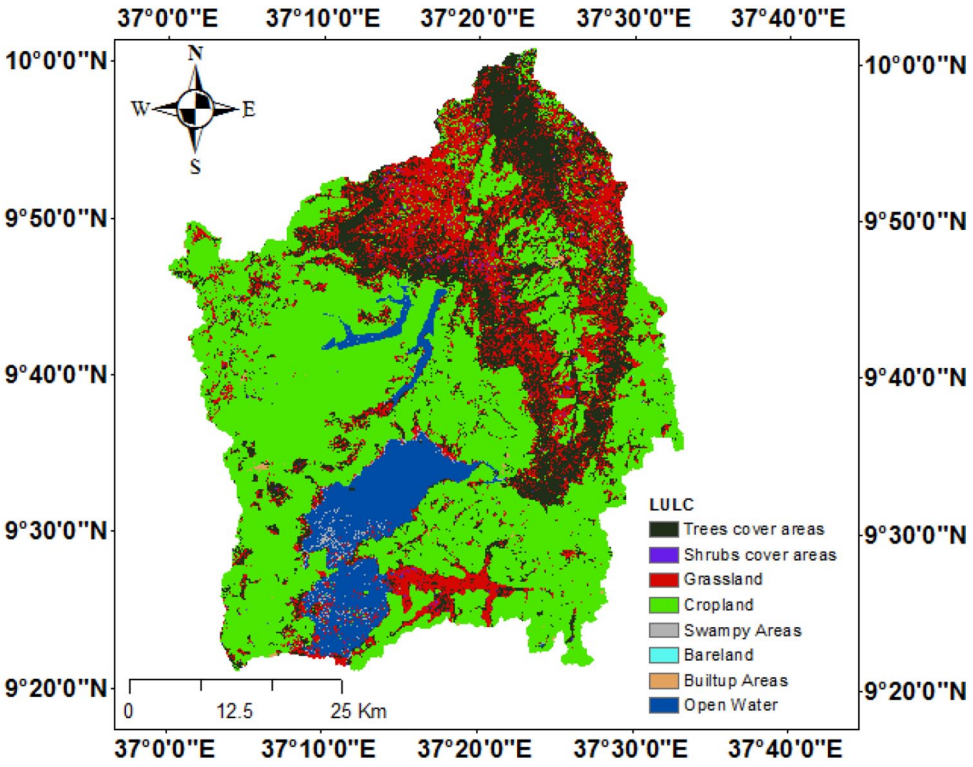

Figure 3. Major Land Use Land Cover (LULC) in the catchment.

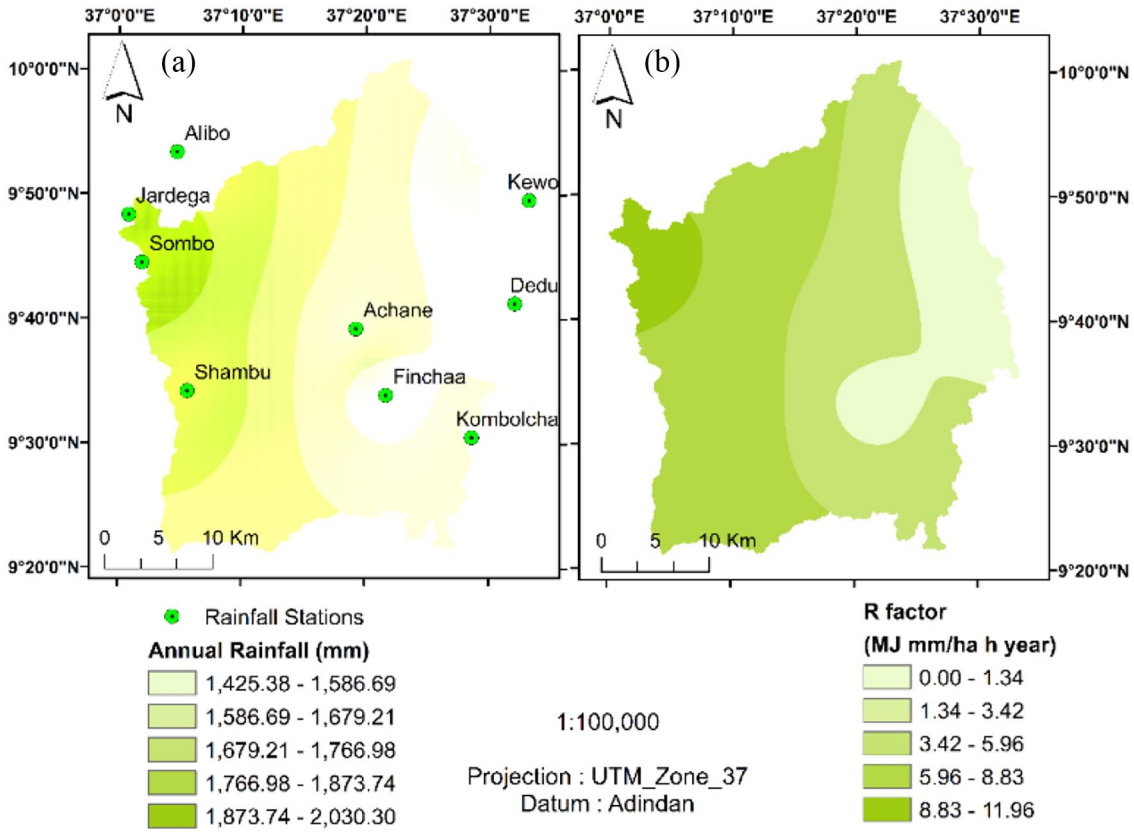

Figure 4. Rainfall classification and derived *R* factor. (a) Existing rainfall categories. (b) R-factor.

Topographic factor (LS)

In a given catchment, the speed and volume of surface run-off are governed by the topographic conditions (Bekele & Gemi, 2021). The topographic factor is the combination of hill-shade (S) and length of the stream (L). The concept behind the importance of the topographic factor (LS) in estimating the soil loss is that the soil erosion increases with

the slope steepness, and the length over which the sensitivity to erosion is valid (Desalegn & Mulu, 2021). The topographic factor (LS) generated from the Digital Elevation Model (DEM) ranges from 0 to 167. The slope length and steepness (LS) increase the velocity of surface runoff causing detachment of soil particles, which in turn lead to erosion. In this catchment, the slope ranges from 0% to 560%, and due to the steepness of the slope, the soil loss is very visible especially for the slope values of more than 11%. As we can see from the Figure 6, the upper portion of the catchment is classified as steep slope whereas the southern part of catchment is low-lying areas. The surface runoff with high velocity is emerged from the upper part of the catchment is causing a severe erosion at the low-lying part of the study area. The ranges of slope (degree) and the corresponding LS-factor values generated in this sudy was presented in Figure 6a and b.

Table 3. Cover and Management (*C*) and Support Practice (*P*) Factors in the Study Area.

LAND USE	*C*-FACTOR VALUE	*P*-FACTOR VALUE
Trees cover areas	0.25	0.27
Shrub cover areas	0.37	0.68
Grass land	0.45	0.87
Crop land	0.68	0.48
Swampy areas	0.75	0.91
Breland	0.65	0.57
Built-up areas	0.47	0.67
Open water	0.66	0.69

Support practice (P) *and cover and management factors*(C)

Soil erosion modeling is also depedent of the surface dynamic changes such as cover and management (*C*) and support practice (*P*). These parameters are used in the Revised Universal Soil Loss Equation (RUSLE) to quantify the annual soil loss. Support and conservation practices factor (P factor) and cover and management factor (C factor) derived from the major LULC (Figure 7) of the catchment are presented in Figure 7a and b respectively. These factors revealed that the lower part of the catchment is sensitive to soil erosion due to the weakness of soil conservation practices (Chalise et al., 2019; Panagos et al., 2015).

The severity of this soil loss was categorized based on the qualitative classification namely; Very Low (red), Low (green), Moderate (yellow), and High (blue) and the corresponding soil loss class was presented in Figure 8a and b respectively.

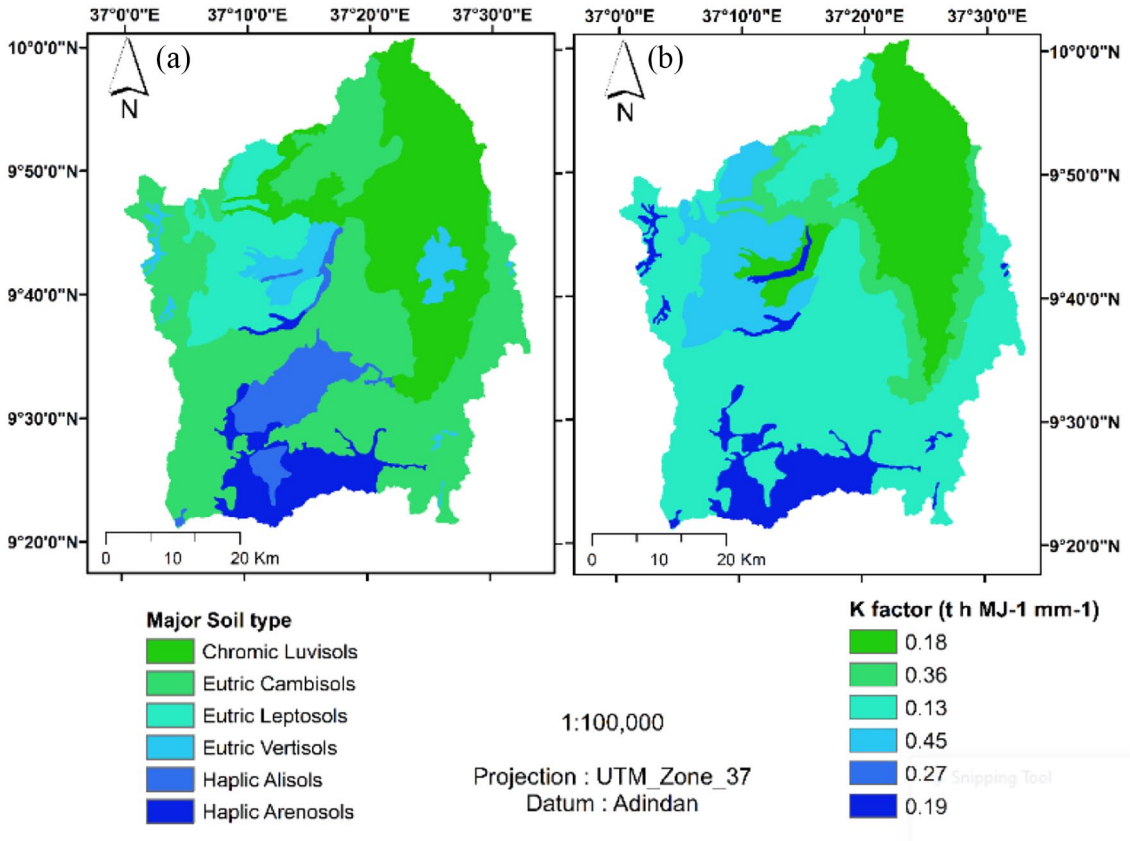

Figure 5. Major soil types and derived *K* factor. (a) Soil categories. (b) K-factor.

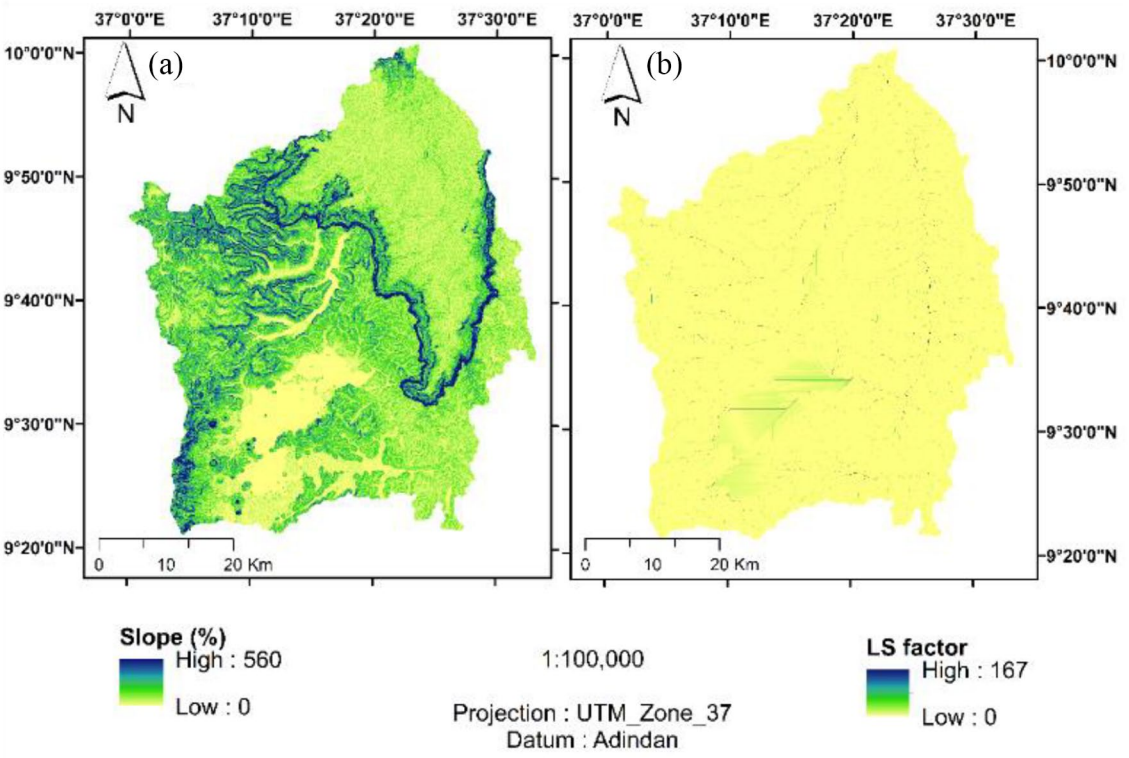

Figure 6. The slope classification and the derived LS factor. (a) Slope categories. (b) LS factor.

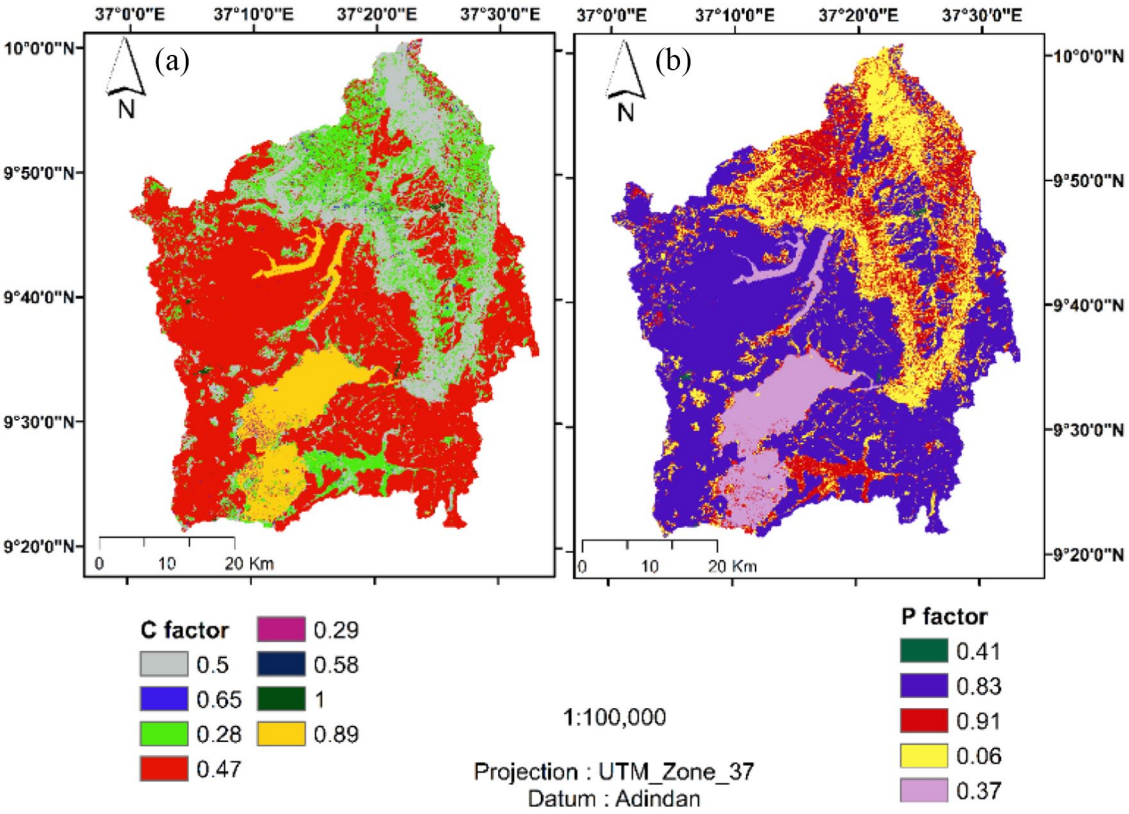

Figure 7. The derived C factor and P factor in the catchment. (a) C factor. (b) P factor.

Although the general rate of annual soil loss in this particular study is classified into four, the degree of severity is different from watershed to watershed. The detailed spatial variability of the soil loss for the individual watershed and the computed percentage of the annual soil loss for each watershed are presented in Table 4.

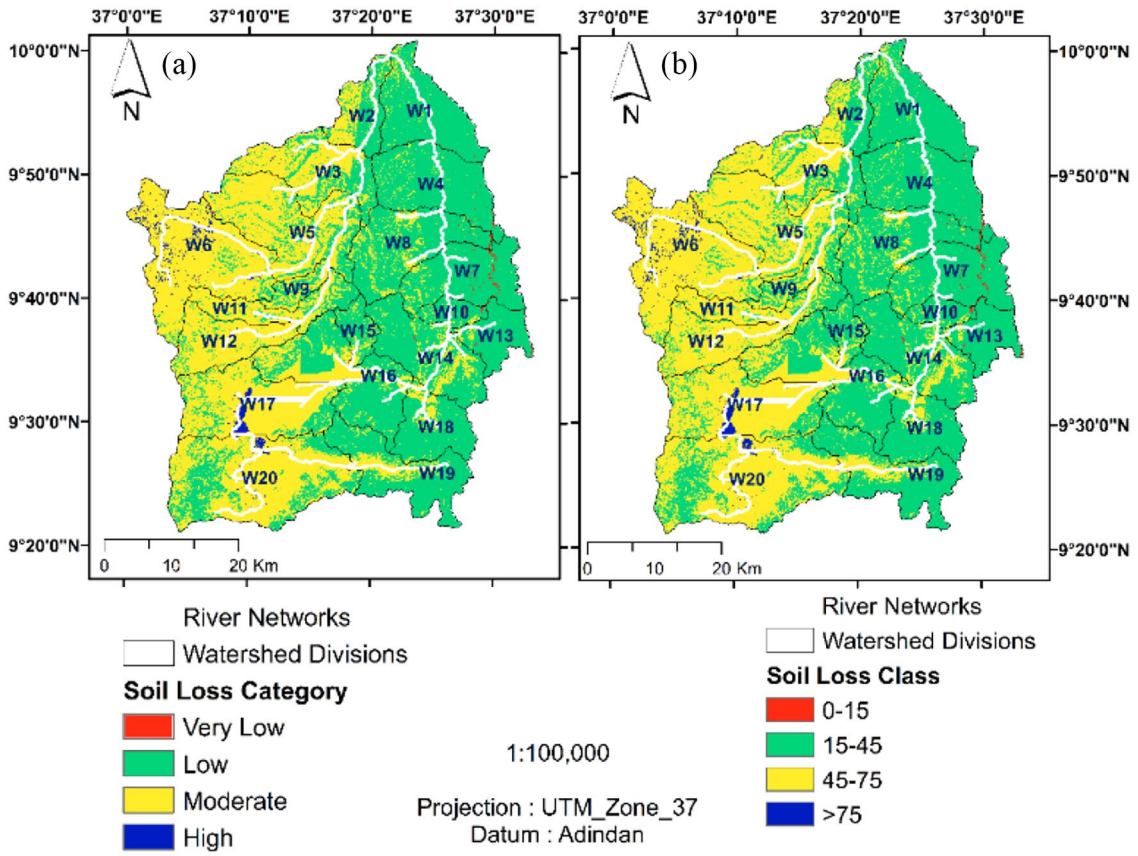

Figure 8. Qualitative based spatial variation of soil erosion severity map in Fincha catchment. (a) Qualitative soil loss categories. (b) Quantitative soil loss categories.

The catchment was distributed and divided into small watershed division labeled as W1, W2, W3. . .. W20. As we can see from Figure 9, the severity for the different soil loss classifications obtained in RUSLE model and the qualitative classification of the soil loss as Very Low (0–15 t ha^{-1} yr^{-1}), Low (15–45 t ha^{-1} yr^{-1}), Moderate (45–75 t ha^{-1} yr^{-1}), and High (>75 t ha^{-1} yr^{-1}) were identified. In terms percentage coverage of soil erosion severity in the catchment, a total eight (those are labeled as W3, W5, W7, W8, W10, W11, W17, and W20) out of twenty of watershed divisions are very vulnerable to the soil erosion as revealed in Table 4 and Figure 10.

The percentage coverage of the soil loss severity for the individual watershed under the qualitative classification is 10%, 15%, 30%, and 45% were identified as very low, Low, moderate, high, respectively. As revealed in the severity map generated in RUSLE model (Figure 10), the cropland and grassland which cover 65% of the total area are highly vulnerable to the soil erosion. The spatial variability of annual soil loss shown in Figure 9 showed that the majority of cropland and grassland in the lower part of the catchment is very sensitive to soil loss and this fact is observed in the detailed severity of each watershed (Figure 10). The spatial variation of the soil loss severity map generated in the RUSLE model has a paramount role to alert land resources managers and all stakeholders in controlling the effects via the implementation of both structural and non-structural mitigations. The results of the RUSLE model can also be further considered along with the catchment for practical soil loss quantification that can help for protection practices.

Conclusion

In this study, the application of an integrated RUSLE model and GIS platforms for the quantification of soil loss in Fincha catchment, Ethiopia is presented. The study divided the Fincha catchment into four soil erosion severity categories; Very Low (0–15 t ha^{-1} yr^{-1}), Low (15–45 t ha^{-1} yr^{-1}), Moderate (45–75 t ha^{-1} yr^{-1}), and High (>75 t ha^{-1} yr^{-1}) and the spatial distribution in each watershed is also presented. In this paper it is also demonstrated that the integration of RUSLE model and GIS platforms is powerful and relevant approaches for quantifying and assessing the spatial distribution of rate of soil loss for effective soil resource management. The soil erosion-prone areas generated in this catchment will support to implement soil conservation measures. From this study, it was found that the upper and the low-lying areas are highly vulnerable to soil erosion and a soil conservation strategy should be implemented to control the loss of top fertile soil in the catchment. Additionally, capacity building training should be given for the farmers and soil conservation experts to minimize the impacts of the erosion. Therefore, having information on the spatial

Table 4. Summary of Soil Loss (ton/yr) and Loss Percentage of Each Watershed.

WATERSHED	SOIL LOSS (TON/YR.)				TOTAL AREA (HA)	PERCENTAGE (SOIL LOSS/TOTAL AREA)			
	0–15TON	15–45TON	45–75TON	>75TON		0–15TON	15–45TON	45–75TON	>75TON
W1	28.11	63.98	82.47	120.27	148.25	81.12	55.63	43.16	18.96
W2	27.06	59.08	79.57	18.15	81.03	22.40	98.20	72.91	33.39
W3	26.76	55.87	76.50	115.42	153.46	75.21	49.85	36.40	17.43
W4	25.71	53.04	73.47	114.79	165.27	69.46	44.45	32.10	15.56
W5	24.68	50.43	70.64	113.33	222.37	50.96	31.77	22.68	11.10
W6	24.39	48.88	68.96	111.87	259.90	43.04	26.53	18.81	9.38
W7	23.51	47.67	67.48	111.66	141.39	78.97	47.72	33.72	16.63
W8	23.37	47.16	66.18	111.45	163.09	68.34	40.58	28.92	14.33
W9	23.66	14.96	15.63	10.20	33.38	30.56	46.82	44.81	70.87
W10	25.27	13.61	23.43	29.99	32.24	93.03	72.66	42.21	78.38
W11	25.57	43.11	63.06	70.41	86.97	80.96	72.51	49.57	29.40
W12	30.57	40.95	63.06	105.01	109.16	96.20	57.77	37.51	28.00
W13	29.94	39.63	63.06	29.47	68.03	43.32	92.70	58.26	44.01
W14	31.49	39.14	63.06	138.79	155.81	89.08	40.47	25.12	20.21
W15	32.43	37.19	32.70	25.51	38.41	66.43	85.13	96.83	84.42
W16	37.21	36.71	60.88	129.89	202.35	64.19	30.09	18.14	18.39
W17	43.96	35.59	62.70	122.18	209.28	58.38	29.96	17.00	21.00
W18	47.52	34.47	62.70	96.89	102.02	94.97	61.46	33.79	46.58
W19	58.58	34.15	60.34	113.53	150.76	75.31	40.02	22.65	38.85
W20	69.16	33.21	58.54	112.49	314.66	35.75	18.60	10.55	21.98
Tot. soil loss	658.91	828.83	1,014.42	1,801.30	2,148				

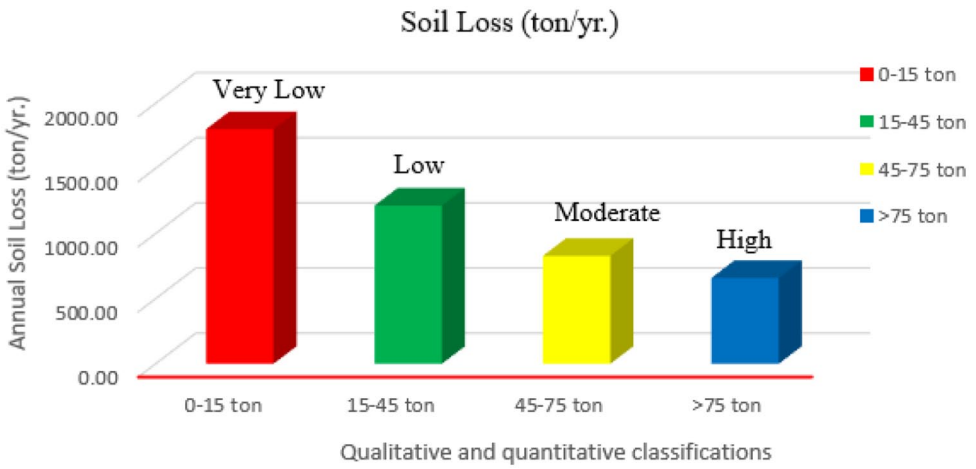

Figure 9. Soil loss class and qualitative classifications.

variability of soil erosion has a paramount role to support land resources managers and all stakeholders in controlling the impacts of the soil erosion. Finally, it was concluded that the results of the RUSLE model can also be further considered along with the catchment for practical soil loss protection practices.

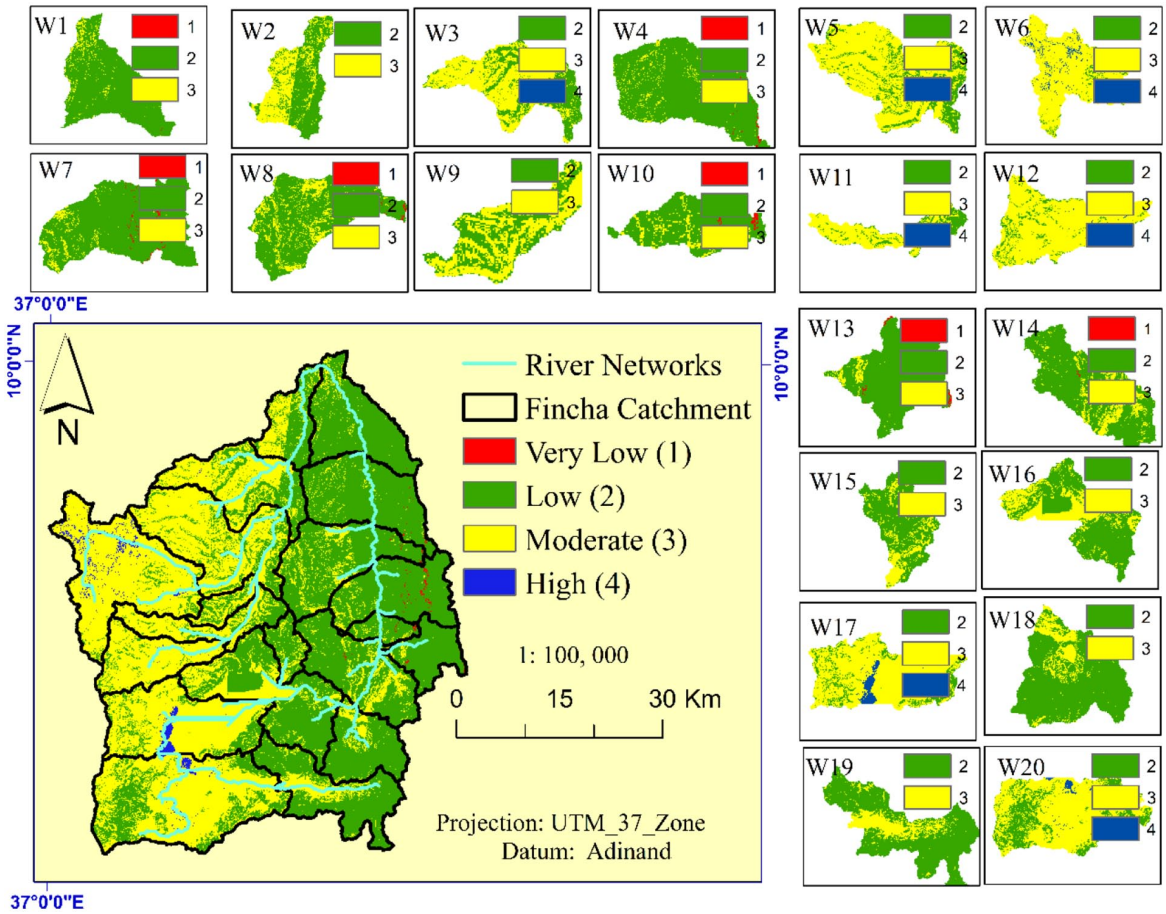

Figure 10. The spatial variability of the soil loss of the individual watershed.

Authors' Contributions

The correspondent author initiated the research idea, reviewed relevant literature, designed the methods, conducted field data collection, performed data cleaning, analyzed the data, interpretation, and prepare draft manuscripts for publication. Co-author evaluated the research idea, supervised the whole research activities, and developed the manuscript. All authors read and approved the final manuscript.

Availability of Data and Material

The data generated and processed in this manuscript were included in the manuscript submission. Further data will be provided up on the request of corresponding author.

Consent for Publication

All authors read the manuscript and agreed to publication.

Declaration of Conflicting Interests

The author(s) declared no potential conflicts of interest with respect to the research, authorship, and/or publication of this article.

Ethics Approval and Consent to Participate

This research paper is part of my community-based project entitled "Natural Resources management strategies."Therefore, all authors approve to publish the findings, and there is no ethical conflict.

Funding

The author(s) received no financial support for the research, authorship, and/or publication of this article.

ORCID iD

Habtamu Tamiru https://orcid.org/0000-0002-2412-6017

REFERENCES

Abdulkadir, T. S., Muhammad, R. U. M., Wan Yusof, K., Ahmad, M. H., Aremu, S. A., Gohari, A., & Abdurrasheed, A. S. (2019). Quantitative analysis of soil erosion causative factors for susceptibility assessment in a complex watershed. *Cogent Engineering*, 6(1), 1594506. https://doi.org/10.1080/23311916.2019.1594506

Ayenew, B., Taddesse, A. M., Kibret, K., & Melese, A. (2018). Chemical forms of phosphorous and physicochemical properties of acid soils of Cheha and Dinsho districts, southern highlands of Ethiopia. *Environmental Systems Research*, 7(1), 1–15. https://doi.org/10.1186/s40068-018-0118-9

Bekele, B., & Gemi, Y. (2021). Soil erosion risk and sediment yield assessment with universal soil loss equation and GIS: In Dijo watershed, Rift valley Basin of Ethiopia. *Modeling Earth Systems and Environment*, 7(1), 273–291. https://doi.org/10.1007/s40808-020-01017-z

Chalise, D., Kumar, L., Spalevic, V., & Skataric, G. (2019). Estimation of sediment yield and maximum outflow using the IntErO model in the Sarada river basin of Nepal. *Water*, 11(5), 952. https://doi.org/10.3390/w11050952

Chuenchum, P., Xu, M., & Tang, W. (2020). Predicted trends of soil erosion and sediment yield from future land use and climate change scenarios in the Lancang–Mekong river by using the modified RUSLE model. *International Soil and Water Conservation Research*, 8(3), 213–227. https://doi.org/10.1016/j.iswcr.2020.06.006

Desalegn, H., & Mulu, A. (2021). Flood vulnerability assessment using GIS at Fetam watershed, upper Abbay basin, Ethiopia. *Heliyon*, 7(1), e05865. https://doi.org/10.1016/j.heliyon.2020.e05865

Dessalegn, T. A., Moges, M. A., Dagnew, D. C., & Gashaw, A. (2017). Applicability of Galway River Flow Forecasting and Modeling System (GFFMS) for Lake Tana Basin, Ethiopia. *Journal of Water Resource and Protection*, 9(12), 1319–1334. https://doi.org/10.4236/jwarp.2017.912084

Dinka, M. O. (2020). Quantification of soil erosion and sediment yield for ungauged catchment using the RUSLE model: Case study for Lake Basaka catchment in Ethiopia. *Lakes & Reservoirs Research & Management*, 25(2), 183–195. https://doi.org/10.1111/lre.12312

Fayas, C. M., Abeysingha, N. S., Nirmanee, K. G. S., Samaratunga, D., & Mallawatantri, A. (2019). Soil loss estimation using rusle model to prioritize erosion control in KELANI river basin in Sri Lanka. *International Soil and Water Conservation Research*, 7(2), 130–137. https://doi.org/10.1016/j.iswcr.2019.01.003

Fenta, A. A., Tsunekawa, A., Haregeweyn, N., Poesen, J., Tsubo, M., Borrelli, P., Panagos, P., Vanmaercke, M., Broeckx, J., Yasuda, H., Kawai, T., & Kurosaki, Y. (2020). Land susceptibility to water and wind erosion risks in the East Africa region. *Science of the Total Environment*, 703, 135016. https://doi.org/10.1016/j.scitotenv.2019.135016

Fernandez, C., Wu, J. Q., McCool, D. K., & Stöckle, C. O. (2003). Estimating water erosion and sediment yield with GIS, RUSLE, and SEDD. *Journal of Soil and Water Conservation*, 58(3), 128–136.

Girmay, G., Moges, A., & Muluneh, A. (2020). Estimation of soil loss rate using the USLE model for Agewmariayam watershed, northern Ethiopia. *Agriculture & Food Security*, 9(1), 1–12. https://doi.org/10.1186/s40066-020-00262-w

Hategekimana, Y., Allam, M., Meng, Q., Nie, Y., & Mohamed, E. (2020). Quantification of soil losses along the coastal protected areas in Kenya. *Land*, 9(5), 137–216. https://doi.org/10.3390/land9050137

Iticha, B., & Takele, C. (2018). Soil-landscape variability: Mapping and building detail information for soil management. *Soil Use and Management*, 34(1), 111–123. https://doi.org/10.1111/sum.12404

Kayet, N., Pathak, K., Chakrabarty, A., & Sahoo, S. (2018). Evaluation of soil loss estimation using the RUSLE model and SCS-CN method in hillslope mining areas. *International Soil and Water Conservation Research*, 6(1), 31–42. https://doi.org/10.1016/j.iswcr.2017.11.002

Li, P. (2018). Groundwater quality in western China: Challenges and paths forward for groundwater quality research in western China. *Exposure and Health*, 8(3), 305–310. https://doi.org/10.1007/s12403-016-0210-1

Markose, V. J., & Jayappa, K. S. (2016). Soil loss estimation and prioritization of sub-watersheds of Kali River basin, Karnataka, India, using RUSLE and GIS. *Environmental Monitoring and Assessment*, 188(4), 225. https://doi.org/10.1007/s10661-016-5218-2

Mengistu, D. T., Moges, S. A., & Sorteberg, A. (2016). Revisiting systems type black-box rainfall-runoff models for flow forecasting application. *Journal of Water Resource and Protection*, 8, 65–83.

Mohamed, C., & Shantha, N. (2019). Soil loss estimation using rusle model to prioritize erosion control in KELANI river basin in Sri Lanka. *International Soil and Water Conservation Research*, 7(2), 130–137. https://doi.org/10.1016/j.iswcr.2019.01.003

Negasa, D. J. (2020). Effects of land use types on selected soil properties in Central Highlands of Ethiopia. *Applied and Environmental Soil Science*, 2020, 1–9. https://doi.org/10.1155/2020/7026929

Olika, G., & Iticha, B. (2019). Assessment of soil erosion using RUSLE and GIS techniques: A case of Fincha'a watershed, western Ethiopia. *Journal of Agriculture and Environmental Sciences*, 19(1), 31–36. https://doi.org/10.5829/idosi.aejaes.2019.31.36

Panagos, P., Borrelli, P., Meusburger, K., Alewell, C., Lugato, E., & Montanarella, L. (2015). Estimating the soil erosion cover-management factor at the European scale. *Land Use Policy*, 48, 38–50. https://doi.org/10.1016/j.landusepol.2015.05.021

Panagos, P., Meusburger, K., Ballabio, C., Borrelli, P., & Alewell, C. (2014). Soil erodibility in Europe: A high-resolution dataset based on LUCAS. *Science of the Total Environment*, 479–480(1), 189–200. https://doi.org/10.1016/j.scitotenv.2014.02.010

Panagos, P., Standardi, G., Borrelli, P., Lugato, E., Montanarella, L., & Bosello, F. (2018). Cost of agricultural productivity loss due to soil erosion in the European Union: From direct cost evaluation approaches to the use of macroeconomic models. *Land Degradation and Development*, 29(3), 471–484. https://doi.org/10.1002/ldr.2879

Phinzi, K., & Silas, N. (2019). The assessment of water-borne erosion at catchment level using GIS-based RUSLE and remote sensing: A review. *International Soil and Water Conservation Research*, 7(1), 27–46. https://doi.org/10.1016/j.iswcr.2018.12.002

Prasannakumar, V., Vijith, H., Abinod, S., & Geetha, N. (2012). Estimation of soil erosion risk within a small mountainous sub-watershed in Kerala, India, using Revised Universal Soil Loss Equation (RUSLE) and geo-information technology. *Geoscience Frontiers*, 3(2), 209–215. https://doi.org/10.1016/j.gsf.2011.11.003

Seifu, W., Elias, E., & Gebresamuel, G. (2020). The effects of land use and landscape position on soil physicochemical properties in a semiarid watershed, northern Ethiopia. *Applied and Environmental Soil Science*, 2020, 1–20. https://doi.org/10.1155/2020/8816248

Shiferaw, M., & Abebe, R. (2020). A spatial analysis and modeling study of sedimentation impacts on dams found in south Gondar zone, Ethiopia. *Modeling Earth Systems and Environment*. Advance online publication. https://doi.org/10.1007/s40808-020-01003-5

Thapa, P. (2020). Spatial estimation of soil erosion using RUSLE modeling: A case study of Dolakha district, Nepal. *Environmental Systems Research*, 9(1), 1–10. https://doi.org/10.1186/s40068-020-00177-2

Wubie, M. A., & Assen, M. (2020). Effects of land cover changes and slope gradient on soil quality in the Gumara watershed, Lake Tana basin of north–west Ethiopia. *Modeling Earth Systems and Environment*, 6(1), 85–97. https://doi.org/10.1007/s40808-019-00660-5

Yan, R., Zhang, X., Yan, S., & Chen, H. (2018). Estimating soil erosion response to land use/cover change in a catchment of the Loess plateau, China. *International Soil and Water Conservation Research*, 6(1), 13–22. https://doi.org/10.1016/j.iswcr.2017.12.002

Yesuph, A. Y., & Dagnew, A. B. (2019). Soil erosion mapping and severity analysis based on RUSLE model and local perception in the Beshillo catchment of the Blue Nile Basin, Ethiopia. *Environmental Systems Research*, 8(1), 1–21. https://doi.org/10.1186/s40068-019-0145-1